Electrochemical Generation and Electron Paramagnetic Resonance Studies of C_{60}^-, C_{60}^{2-}, and C_{60}^{3-}

Mazen M. Khaled, Richard T. Carlin,† Paul C. Trulove,† Gareth R. Eaton, and Sandra S. Eaton*

Contribution from the Department of Chemistry, University of Denver, Denver, Colorado 80208, and Frank J. Seiler Research Laboratory, US Air Force, Academy, Colorado 80840

Received December 13, 1993®

Abstract: The -1, -2, and -3 anions of C_{60} were generated electrochemically in 4:1 toluene-acetonitrile. The visible/near-IR spectra were monitored in situ. Square wave voltammograms and electronic spectra showed that after bulk electrolysis to produce the anions, the following percentages of the starting C_{60} concentration could be reoxidized to neutral C_{60} in typical data sets: -1 anion, 75%; -2 anion, 66%; -3 anion, 46%. Continuous wave (CW) electron paramagnetic resonance (EPR) spectra of the -1 and -3 anions exhibited broad signals that were temperature dependent. The averaging of anisotropy of the signals between 15 and 60 K is attributed to dynamic Jahn-Teller distortion. Electron spin-echo and saturation recovery EPR data for the -1 anion at 10 and 16 K showed that the electron spin relaxation rates are dependent upon position in the spectrum, which is attributed to variations in the Jahn-Teller distortion. For both the -1 and -3 anion above about 70 K the CW line shape of the EPR signal is electron spin-lattice relaxation rate determined. The EPR data indicate that the -2 anion is diamagnetic. The sharp signals that are observed with varying intensity in the spectra of the -1, -2, and -3 anions have much slower electron spin-lattice relaxation rates than the signals for the -1 and -3 anions. The line shapes for the sharp signal(s) are largely independent of temperature. These signals are assigned to as-yet unidentified species with lower symmetry and slower molecular rotation than the C_{60} anions.

Introduction

The high symmetry, the fascination with a new form of carbon, the possibility of superconducting derivatives, and the availability in sufficient quantities for preparative work have led to extensive work on C_{60} by many groups.[1] Early molecular orbital calculations showed that the LUMO for C_{60} is triply degenerate,[2-5] and electrochemical experiments have demonstrated reduction of C_{60} by 1 to 6 electrons, populating the LUMO.[6,7] Electron paramagnetic resonance (EPR) studies have been reported for the -1, -2, and -3 anions,[8-19] but questions remain concerning the assignment of some of the EPR signals. One of the major questions concerns the nature of the dianion. Molecular orbital calculations predict that the anions are subject to Jahn-Teller distortion, removing the degeneracy of the LUMO and producing a diamagnetic dianion.[20,21] However, the observation of an EPR signal for solutions containing the dianion has led some to conclude that the dianion is paramagnetic with $S = 1$.[8,13,16,19] An interpretation of the visible/near-IR (vis/NIR) spectra is consistent with an $S = 1$ state for the dianion.[22] One of the difficulties in interpreting the bulk electrolysis data and EPR spectra of C_{60}^{n-} is the lack of information concerning the reversibility of the anion formation on the time scale of the bulk electrolysis and the lack of quantitation of the EPR spectra. In the following paragraphs we report experiments designed to address these issues.

Experimental Section

C_{60} was purchased from SES Research (Houston, TX) and used without further purification. Tetrabutylammonium hexafluorophosphate ($TBAPF_6$) (electrochemical grade, Fluka) was dried overnight in a vacuum oven at 110 °C. Anhydrous acetonitrile and toluene (<0.005% H_2O, Aldrich) were kept over 4 Å molecular sieves (dried for 24 h at 400 °C, 10^{-6} Torr) for several hours prior to use. Traces of water from the solvent and/or supporting electrolyte may be a source of lab-to-lab variation in results.

Electrochemistry was done at the Seiler Research Laboratory and EPR was done at the University of Denver. Square wave voltammetry (SWV) and bulk electrolysis were performed using an EG&G Princeton Applied Research (PAR) Model 273 potentiostat/galvanostat interfaced to a personal computer running the PAR 270 software. Solutions for electrochemistry were 0.2 to 0.3 mM C_{60} in an electrochemical solvent composed of 4:1 (v/v) toluene-acetonitrile with 0.1 M $TBAPF_6$. A three-electrode cell was used for all electrochemical studies. For square wave voltammetry (SWV), the working electrode was a 3 mm glassy carbon

† US Air Force.

• Abstract published in *Advance ACS Abstracts*, March 15, 1994.

(1) Kroto, H. W.; Fischer, J. E.; Cox, D. E., Ed. *The Fullerenes*; Pergamon Press: Oxford, 1993.
(2) Bochvar, D. A.; Gal'pern, E. G. *Dokl. Akad. Nauk SSSR* **1973**, *209*, 610.
(3) Haddon, R. C.; Brus, L. E.; Raghavachari *Chem. Phys. Lett.* **1986**, *125*, 459.
(4) Haymet, A. D. J. *Chem. Phys. Lett.* **1985**, *122*, 421.
(5) Disch, R. L.; Schulman, J. M. *Chem. Phys. Lett.* **1986**, *125*, 465.
(6) Xie, Q.; Perez-Cordero, E.; Echegoyen, L. *J. Am. Chem. Soc.* **1992**, *114*, 3978. References to the earlier work on electrochemistry of C_{60} are cited here.
(7) Ohsawa, Y.; Saji, T. *J. Chem. Soc. Chem. Commun.* **1992**, 781.
(8) Stinchcombe, J.; Penicaud, A.; Bhyrappa, P.; Boyd, P. D. W.; Reed, C. A. *J. Am. Chem. Soc.* **1993**, *115*, 5212.
(9) Schell-Sorokin, A. J.; Mehran, F.; Eaton, G. R.; Eaton, S. S.; Viebeck, A.; O'Toole, T. R.; Brown, C. A. *Chem. Phys. Lett.* **1992**, *195*, 225.
(10) Mehran, F.; Schell-Sorokin, A. J.; Brown, C. A. *Phys. Rev. B* **1992**, *46*, 8579.
(11) Allemand, P.-M.; Srdanov, G.; Koch, A.; Khemani, K.; Wudl, F.; Rubin, Y.; Diedrich, F.; Alvarez, M. M.; Anz, S. J.; Whetten, R. L. *J. Am. Chem. Soc.* **1991**, *113*, 2780.
(12) Keizer, P. N.; Morton, J. R.; Preston, K. F.; Sugden, A. K. *J. Phys. Chem.* **1991**, *95*, 7117.
(13) Dubois, D.; Jones, M. T.; Kadish, K. M. *J. Am. Chem. Soc.* **1992**, *114*, 6446.
(14) Moriyama, H.; Kobayashi, H.; Kobayashi, A.; Watanabe, T. *J. Am. Chem. Soc.* **1993**, *115*, 1185.
(15) Boulas, P.; Subramanian, R.; Kutner, W.; Jones, M. T.; Kadish, K. M. *J. Electrochem. Soc.* **1993**, *140*, L130.
(16) Baumgarten, M.; Gugel, A.; Gherghel, L. *Adv. Mater.* **1993**, *5*, 458.
(17) Greaney, M. A.; Gorun, S. M. *J. Phys. Chem.* **1991**, *95*, 7142.
(18) Bossard, C.; Rigaut, S.; Astruc, D.; Delville, M.-H.; Felix, G.; Fevrier-Bouvier, A.; Amiell, J.; Flandrois, S.; Delhaes, P. *J. Chem. Soc., Chem. Commun.* **1993**, 333.
(19) Dubois, D.; Kadish, K. M.; Flanagan, S.; Haufler, R. E.; Chibante, L. P. F.; Wilson, L. J. *J. Am. Chem. Soc.* **1991**, *113*, 4364.
(20) Koga, N.; Morokuma, K. *Chem. Phys. Lett.* **1992**, *196*, 191.
(21) Adams, G. B.; Sankey, O. F.; Page, J. B.; O'Keeffe, M. *Chem. Phys.* **1993**, *176*, 61.
(22) Lawson, D. R.; Feldheim, D. L.; Foss, C. A.; Dorhout, P. K.; Elliott, C. M.; Martin, C. R.; Parkinson, B. *J. Electrochem. Soc.* **1992**, *139*, L68.

0002-7863/94/1516-3465$04.50/0

(GC) electrode from Bioanalytical Systems. For bulk electrolysis, the working electrode was a coil of 0.5 mm diameter Pt wire. The counter and reference electrodes were the same for all experiments. The counter electrode was a Pt wire contained in a 5 mm OD Ace Glass gas dispersion tube (D porosity) filled with electrochemical solvent. This gas dispersion tube was inserted into a side-arm compartment of the electrolysis cell which contacted the electrolysis solution through a heat-constricted fine glass frit. The Ag/Ag^+ reference potential was established using a Ag wire immersed in acetonitrile containing 0.01 M $AgNO_3$. The reference electrode solution was contained in a 3 mm OD Pyrex tube with a porous vycor plug sealed to one end. This tube was then inserted into a 7 mm OD Ace Glass gas dispersion tube (E porosity) which dipped into the electrolysis solution. The double junction arrangement for both the counter and reference electrodes minimized contamination of the electrolysis solution during the several hours required for bulk electrolysis. All of the electrochemical experiments were done at room temperature, which was about 20 °C.

Electrochemistry and EPR sample preparation were performed in a Vacuum Atmospheres drybox with O_2 and H_2O concentration less than 1 ppm. Optical spectra were obtained *in situ* via a fiber optic dip probe connected to a Guided Wave Model 260 spectrometer. The optical cables were run through the wall of the drybox using a homemade gas-tight seal. The optical path length for the cell was 0.40 cm. Samples for EPR spectroscopy were withdrawn from the electrolysis cell with a syringe, loaded into 4 mm OD quartz EPR tubes, and capped with pinch-clamped tygon tubing. The capped samples were removed from the glovebox and placed in a dewar of liquid nitrogen within 10 min after stopping electrolysis. The frozen EPR samples were rapidly transported to a vacuum line where they were evacuated and then sealed with a torch. Samples were stored in liquid nitrogen until EPR spectra were recorded. During all manipulations subsequent to removal from the glovebox, except as specifically noted in conditions for obtaining spectra, the samples were maintained at liquid nitrogen temperatures to minimize reaction of the anions with solvent or trace impurities.

Two-pulse electron spin–echo and saturation recovery experiments were performed on the locally-constructed spectrometers that have been described in the literature.[23,24] CW (continuous wave) EPR spectra were recorded on an IBM/Bruker ER200D or in the CW mode of the spin–echo or saturation recovery spectrometers. Data were obtained at frequencies between 9.2 and 9.5 GHz and were collected into PC-style computers for storage and analysis. Temperatures below 77 K were obtained with an Oxford ESR900 flow cryostat. Temperatures above 77 K were obtained with a cooled nitrogen flow cryostat. Temperatures were calibrated by substitution of a thermocouple in a sample tube in place of the EPR sample. Values of the electron spin phase memory time, T_m, were calculated by fitting the spin–echo data to a single exponential of the form $y(t) = y(0)\exp(-t/T_m)$. Saturation recovery data were fit to a single exponential or to the sum of two exponentials using the algorithm of Provencher.[25]

Quantitation of EPR spectra used the stable nitroxyl radical 4-hydroxyl-2,2,6,6-tetramethylpiperidin-1-oxyl (Aldrich Chemical) as the standard. Double integrations of the C_{60} anion spectra were compared with spectra of the standard at 116 K. This temperature was used because the relaxation rate of the nitroxyl standard becomes so slow at lower temperatures that it is difficult to obtain unsaturated spectra. Microwave frequencies were measured with frequency counters. Magnetic field was measured with a gaussmeter or calculated from the known g value of DPPH (2.0036) and the measured microwave frequency. The uncertainty in g values is about ±0.001, due to overlapping lines.

Square Wave Voltammetry of C_{60}. The square wave voltammogram (SWV) of a 0.23 mM solution of C_{60} in 4:1 (v/v) toluene–acetonitrile at a glassy carbon (GC) electrode is shown in Figure 1. Five reduction processes are clearly resolved and are assigned to the generation of the −1, −2, −3, −4, and −5 anions of C_{60}.[6,7] The first four waves were fit using the COOL algorithm to an EEEE electrochemical mechanism (Figure 1) in which each electrochemical step is assumed to be a reversible process.[26] The $E_{1/2}$ values obtained from the fit are −0.850, −1.276, −1.776, and −2.252 V; all values have a 95% confidence limit of ±0.002 V. The values are in good agreement with previously reported reductions

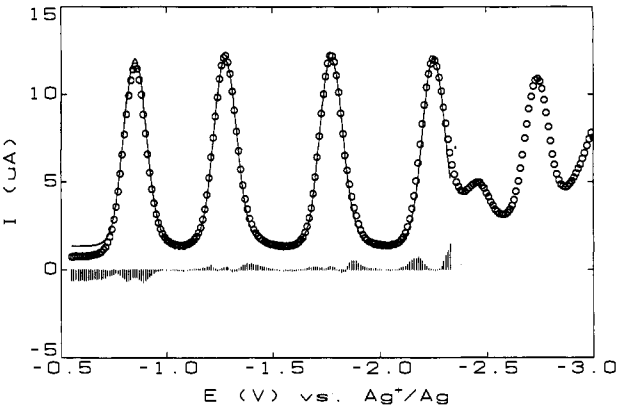

Figure 1. Square wave voltammogram (SWV) of 0.23 mM C_{60} in 4:1 toluene–acetonitrile containing 0.1 M $TBAPF_6$ at a glassy carbon electrode showing experimental data (O) and fit to an EEEE electrochemical mechanism. The lower trace shows the deviation between the observed and calculated curves. Step increment = 10 mV, square wave amplitude = 50 mV, frequency = 10 Hz.

of C_{60},[6,7] taking $E_{1/2}(Fc/Fc^+) = 0.074$ V relative to Ag/Ag^+.[27] The quality of the fit confirms that the first four electrochemical processes are reversible on the time scale of the experiment, which is consistent with the recently reported standard rate constants of 0.46 (1,2-dichlorobenzene) and 0.12 cm s^{-1} (benzonitrile) for reduction of C_{60} to C_{60}^-.[28] We did not attempt to fit the −4/−5 couple at $E_{1/2} = -2.74$ V. The minor reduction wave at −2.46 V was apparent in other C_{60} solutions and may be due to an electroactive impurity in the C_{60} starting material.

To evaluate the stability of the fullerene anions on a short time scale, each anion was generated at a 3-mm GC electrode using an initial 60-s hold at the appropriate potential, and then the potential was scanned positive to reoxidize the anion back to neutral C_{60}. In these scans the observation of individual, well-shaped oxidation waves is evidence of anion stability. Figure 2 summarizes this series of experiments. Block 1 of Figure 2 shows the five reduction steps for C_{60}. Successive blocks show the results of reoxidation after formation of the −1 to −5 anions, respectively. Even for the reoxidation of the −5 anion (block 6), the oxidation peaks mirror the reduction peaks shown in block 1, although an approximate 20–30% decrease in peak height is observed for several of the voltammograms. The peak for the oxidation of C_{60}^- to C_{60} is somewhat of an anomaly in that C_{60}^- appears fully stable in the block 2 voltammogram, yet the peak height is significantly decreased in blocks 3 to 6. It seems unlikely that this behavior indicates poor stability of the −1 anion, because the data in block 2 and the spectroelectrochemistry discussed below indicate the stability of C_{60}^-. In the reoxidations where the −1/0 current is less than that for −1/−2 there is also a broad feature at ca. −0.2 V. When these solutions are subsequently reduced, the 0/−1 and −1/−2 currents are again comparable.

Generation and in Situ Monitoring of C_{60} Anions. Fullerene anions were generated at a coil of Pt wire and the progress of the bulk electrolysis was monitored *in situ* using a fiber optic dip probe operating in the visible and near-IR regimes. The spectral changes observed during the reduction of 0.27 mM C_{60} to C_{60}^- at a potential of −1.03 V are shown in Figure 3. The final spectrum is in good agreement with previous reports[9,16,17,22,29-31] for C_{60}^-. The value of ϵ for the peak at 1075 nm has been reported for a range of solvents and temperatures as 1.2×10^4,[22,30] 1.55×10^4,[29] and 2.0×10^4.[9,10] Using a value of 2.0×10^4,[9,10] the maximum absorbance in Figure 3 corresponds to a C_{60}^- concentration of 0.21 mM, or 78% of the starting C_{60}. At this point the electrolysis was stopped and a sample was withdrawn for EPR spectroscopy.

Further electrolysis at −1.5 V led to conversion of C_{60}^- to C_{60}^{2-} with spectral changes as shown in Figure 4. The peaks at 840 and 950 nm

(23) Quine, R. W.; Eaton, G. R.; Eaton, S. S. *Rev. Sci. Instrum.* **1987**, *58*, 1709.
(24) Quine, R. W.; Eaton, S. S.; Eaton, G. R. *Rev. Sci. Instrum.* **1992**, *63*, 4251.
(25) Provencher, S. W. *Biophys. J.* **1976**, *16*, 27, Provencher, S. W. *J. Chem. Phys.* **1976**, *64*, 2772.
(26) O'Dea, J.; Osteryoung, J.; Lane, T. *J. Phys. Chem.* **1986**, *90*, 2761.
(27) Kolthoff, I. M.; Thomas, F. G. *J. Phys. Chem.* **1965**, *69*, 3049.
(28) Mirkin, M. V.; Bulhoes, L. O. S.; Bard, A. J. *J. Am. Chem. Soc.* **1993**, *115*, 201–204.
(29) Kato, T.; Kodama, T.; Shida, T. *Chem. Phys. Lett.* **1993**, *205*, 405.
(30) Heath, G. A.; McGrady, J. E.; Martin, R. L. *J. Chem. Soc. Chem. Commun.* **1992**, 1272.
(31) Kato, T.; Kodama, T.; Oyama, M.; Okazaki, S.; Shida, T.; Nakagawa, T.; Matsui, Y.; Suzuki, S.; Shiromaru, H.; Yamauchi, K.; Achiba, Y. *Chem. Phys. Lett.* **1991**, *186*, 35.

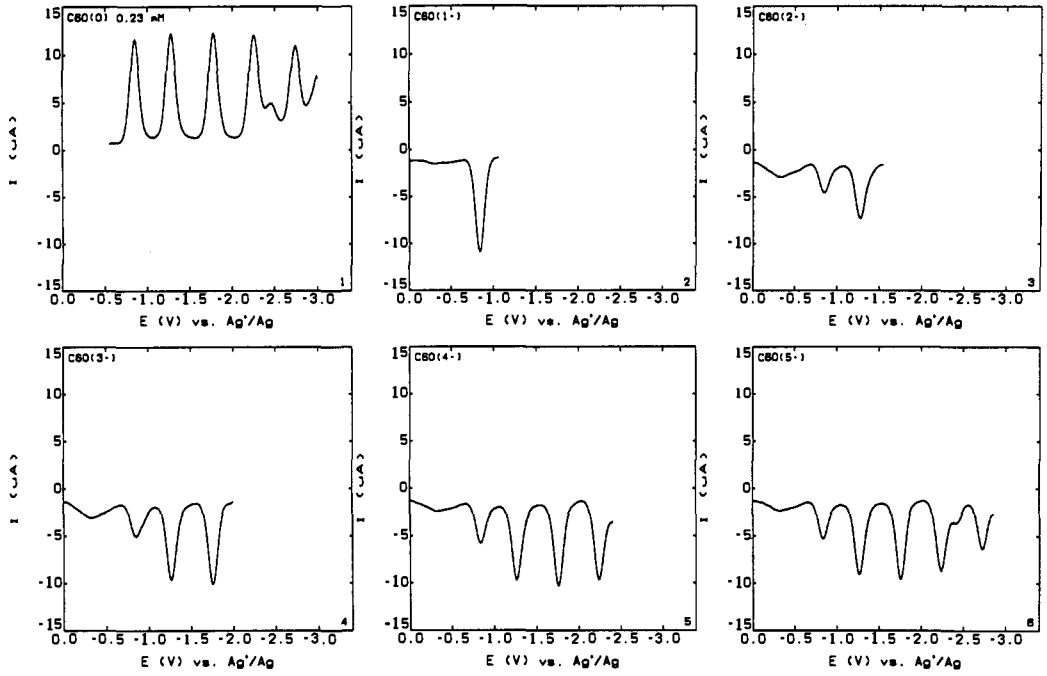

Figure 2. SWV at the GC electrode for (1) reduction of 0.23 mM C_{60} in toluene–acetonitrile and oxidation of (2) C_{60}^-, (3) C_{60}^{2-}, (4) C_{60}^{3-}, (5) C_{60}^{4-}, and (6) C_{60}^{5-}. Anions were generated at the electrode surface by holding at the appropriate reduction potential for 60 s. Step increment = 10 mV, SW amplitude = 50 mV, frequency = 10 Hz.

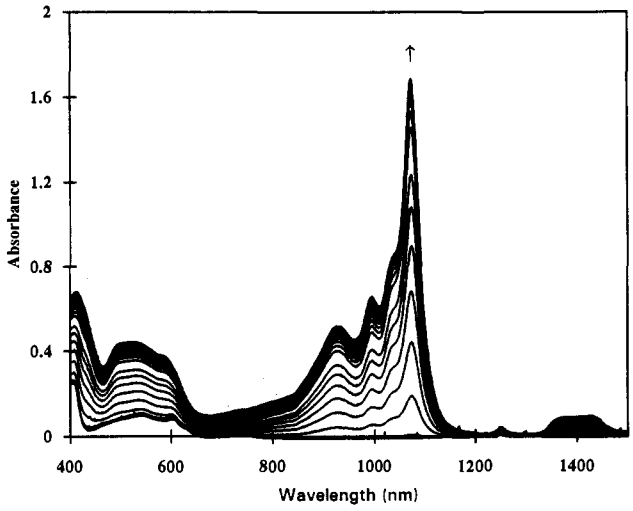

Figure 3. Vis/NIR spectroelectrochemistry for reduction of 0.27 mM C_{60} to C_{60}^- in toluene–acetonitrile containing 0.1 M $TBAPF_6$. The elapsed time for the electrolysis was 105 min.

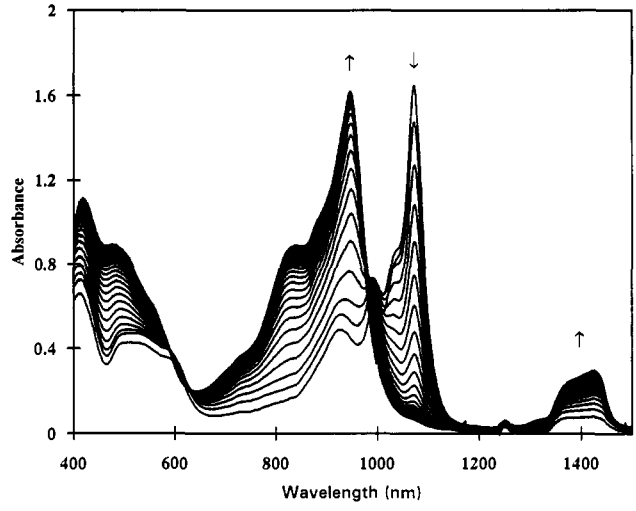

Figure 4. Vis/NIR spectroelectrochemistry for reduction of C_{60}^- to C_{60}^{2-} in toluene–acetonitrile containing 0.1 M $TBAPF_6$. The elapsed time for the electrolysis was 110 min. The spectral changes were reversible, indicating stability of C_{60}^- and C_{60}^{2-}.

in the spectrum of C_{60}^{2-} are in good agreement with the literature.[10,16,22,30,32] On the basis of $\epsilon = 1.85 \times 10^4$ at 950 nm,[10,30] the maximum absorbance for C_{60}^{2-} in Figure 4 corresponds to 0.22 mM C_{60}^{2-}, which is 78% of the initial C_{60}. Baumgarten et al. reported an additional peak in the spectrum of C_{60}^{2-} at 1305 nm,[16] which was not observed in ref 30 or in Figure 4. This peak may be due to an additional species present in their sample.

The spectral changes that occurred during the reduction of C_{60}^{2-} to C_{60}^{3-} at –1.84 V are shown in Figure 5. The spectra obtained for C_{60}^{3-} in repeat experiments were less reproducible than for the –1 and –2 anions. Literature spectra of C_{60}^{3-} also exhibit more variability[16,22,30,32] than the spectra for the –1 and –2 anions, but the intensity observed in Figure 5 between about 720 and 880 nm is typical of what has been reported for C_{60}^{3-}. The C_{60}^{3-} spectrum may be sensitive to the amount and type of impurities formed during the electrolysis. The absorption centered at 1400 nm was present in the spectra for the –1, –2, and –3 anions (Figures 3–5) and increased in the order –1 < –2 < –3. Baumgarten et al.[16] and Lawson et al.[22] observed intensity at 1340 and 1367 nm, respectively, that was assigned to C_{60}^{3-}. Heath et al.[30] observed intensity at 1350 nm for C_{60}^{3-} in CH_2Cl_2, but not in pyridine solution. The fact that the absorption at about 1400 nm appears in spectra of all three anions (Figure 3–5) suggests that it is due to another species produced by the electrolysis. The possibility that it is due to a substituted C_{60} is discussed below. The value of $\epsilon = 1.4 \times 10^4$ at 788 nm[22] was used to estimate the concentration of C_{60}^{3-} in the solutions. The time dependence of the spectra indicated that degradation of the anions was occurring at the potential used to generate C_{60}^{3-}, suggesting that C_{60}^{3-} is less stable than the –1 and –2 anions, which is consistent with a prior report.[19]

To corroborate the spectral results, square wave techniques were employed to determine the total C_{60} concentration remaining after each electrolysis step and to check for the presence of electroactive degradation products. This analysis employed a 3 mm GC electrode and consisted of holding the potential at –0.5 V for about 20 s to convert the anions back to the neutral C_{60} near the electrode surface only, followed by scanning to negative potentials. The resulting "regeneration" voltammogram was compared with the initial C_{60} reduction taking note of peak heights, the appearance of new waves, and the distortion of the original reduction

(32) Fullagar, W. K.; Gentle, I. R.; Heath, G. A.; White, J. W. *J. Chem. Soc., Chem. Commun.* **1993**, 525.

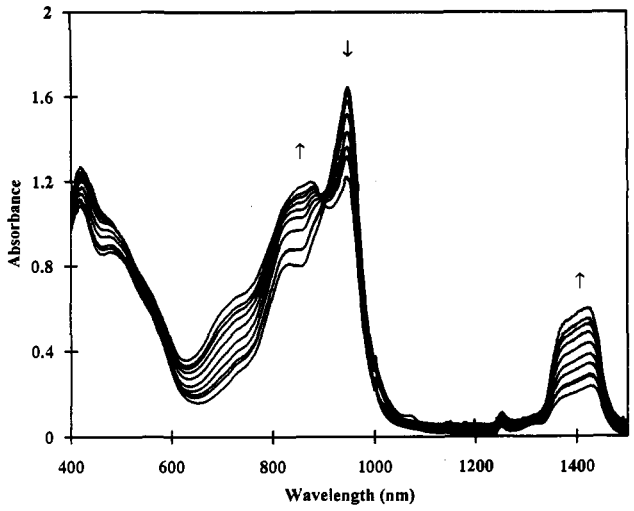

Figure 5. Vis/NIR spectroelectrochemistry for the reduction of C_{60}^{2-} to C_{60}^{3-} in toluene–acetonitrile containing 0.1 M $TBAPF_6$. The elapsed time for the electrolysis was 110 min. Spectra for C_{60}^{3-} were variable, indicating degradation of the C_{60} anions during electrolysis at this potential.

waves. The anion concentration was calculated using the formula:

$$[\text{anion}] = [C_{60}]_i \times (\text{APH after})/(\text{APH before}) \quad (1)$$

where APH is the average of the peak heights for the first three reductions, after refers to data taken after electrolysis, and before refers to data taken on the fresh solution. For the same solution for which the vis/NIR data are shown in Figure 3–5, a series of regeneration voltammograms are shown in Figure 6 and blocks 1, 4, and 7 of Figure 7, following electrolysis to the –1, –2, and –3 anions.

Anion concentrations calculated using eq 1 and data shown in Figure 6 were the following: C_{60}^-, 0.19 mM (72%); C_{60}^{2-}, 0.15 mM (55%); C_{60}^{3-}, 0.14 mM (52%). These values are in reasonable agreement with the values calculated above from the vis/NIR spectra: C_{60}^-, 78%; C_{60}^{2-}, 78%; and C_{60}^{3-}, 40%. This agreement is typical of the bulk electrolysis experiments. In both measurements, overlap of peaks from degradation products with those from the desired anions may cause uncertainties in the estimated concentrations. There also is uncertainty in the ϵ values used to convert absorbance in the vis/NIR spectra to concentration.

In addition to the regeneration voltammograms, following each step in the bulk electrolysis, positive and negative SW voltammograms were collected for each anion, starting at the open circuit potential, to evaluate the electrochemical properties of the anion solutions. The results of the regeneration analyses and the positive/negative scans from the open circuit are presented in Figure 7 for the –1, –2, and –3 anions generated from the 0.27 mM C_{60} solution used for Figure 6.

From Figures 6 and 7, it is apparent that the –1 and –2 anions can be generated relatively cleanly, and in good yield; however this is not the case for the –3 anion. Instead generation of the –3 anion by bulk electrolysis leads to irreversible loss of C_{60} and to the production of electroactive degradation products.

Even the production of the –1 and –2 anions is not quantitative. The anions may react with trace impurities in the solvent, forming substituted C_{60}. For example, it has been shown that C_{60}^{2-} reacts with CH_3I to produce $(CH_3)_2C_{60}$.[33] Reduction of these substituted molecules may be the source of some of the unidentified signals in the EPR spectra. In Figure 8 the voltammogram for reduction of a fresh solution of C_{60} is superimposed on those for samples after bulk electrolysis to produce C_{60}^{3-} followed by re-oxidation to C_{60}^-. After the bulk electrolysis the material in the immediate vicinity of the electrode was re-oxidized by holding the electrode at –0.55 V for 20 s before recording the reduction potentials. After bulk electrolysis to form C_{60}^{3-}, the currents for the production of the –1 to –3 anions were reduced relative to that observed for the initial solution (Figure 8). However, part of that intensity was re-gained after bulk electrolysis to form C_{60}^-. It appears that the electrolysis to form C_{60}^{3-} results in chemical changes of which some can be reversed by bulk oxidation and others are irreversible.

(33) Caron, C.; Subramanian, R.; D'Souza, F.; Kim, J.; Kutner, W.; Jones, M. T.; Kadish, K. M.; *J. Am. Chem. Soc.* **1993**, *115*, 8505.

EPR Spectra of C_{60}^-. CW EPR spectra of C_{60}^- as a function of temperature and microwave power are shown in Figure 9. At 16 K the spectrum is anisotropic and similar to that which has been reported previously at 2.2–15 K.[8,9,29,34] For both high and low microwave powers at 16 K, the high-field wing of the signal is much broader than would be expected based on the line widths of the rest of the spectrum. Spectra at 6 K (not shown) are similar to those at 16 K. Attempts to simulate these spectra as simple axial powder patterns are in poor agreement with the observed line shape (Figure 9), which is consistent with the observations of Reed and co-workers.[8] The simulations do not match the intensity in the high-field wing of the spectrum. As the temperature is increased to 45 or 60 K, the intensity in the high-field wing of the signal moves in toward the center of the spectrum and the extrema marked 2 and 3 (Figure 9) move closer together. As the temperature is increased above about 60 K, the signal broadens as reported previously.[8,9–14,35,36]

Integrated intensities of the EPR spectra of C_{60}^- correspond to concentrations between 25 and 100% of the initial C_{60} concentration. The square wave and visible spectroscopy data for the same samples indicated C_{60}^- concentrations between 45 and 80% of the starting C_{60} concentration. The electrochemical experiment that showed the cleanest conversion to C_{60}^- also gave the EPR signal with the highest integrated intensity. The broad signals for C_{60}^- may introduce some uncertainty in the double integrals; however the concentration obtained from the EPR signal intensity is similar to that calculated by other techniques, consistent with assignment of the broad signal to C_{60}^-.

Electron spin–echo data were obtained for C_{60}^- at 16 K as a function of position in the spectrum (Figure 10). The phase memory relaxation rate, $1/T_m$, was substantially faster in the high-field wing of the spectrum than through the rest of the line. The proton modulation observed was weak, consistent with assignment to solvent protons in the vicinity of the anion.

Saturation recovery was used to measure T_1 for the anion as a function of position in the spectrum (Figure 11). The spin–lattice relaxation rate ($1/T_1$) was strongly dependent on position in the line, with the fastest relaxation rates observed at the high-field end of the spectrum. A similar variation in $1/T_1$ was observed at 10 K, although rates were slower by about a factor of 4 than at 16 K. In addition to the variation in relaxation rate through the spectrum, there was a wide distribution in relaxation rates at each point in the spectrum. Fits of the saturation recovery data to the sum of two exponentials gave two contributions that differed by about an order of magnitude in T_1. It has been noted that with noise-containing experimental data one cannot distinguish between a sum of discrete exponentials and a distribution of exponentials centered at the mean value of the discrete exponentials.[37,38] Although the data were fit to a sum of two exponentials, this probably is a surrogate for a distribution of exponentials. The saturation recovery spectrometer uses a Varian TE_{102} resonator with a loaded Q of about 3000. The value of Q limits the range of magnetic fields that is examined in an individual saturation recovery experiment to about 1 G. Thus the distribution is not due to the simultaneous detection of signals from a range of magnetic fields. In a flow cryostat there is a distribution of temperatures over the length of the sample, which in this case may be 1–2 K. The present data at 10 and 16 K and the previous study of the temperature dependence of T_1[9] show that the observed distribution in T_1 is larger than can be explained on the basis of the temperature variation over the sample.

At 16 K and low microwave power (0.8×10^{-3} mW) (Figure 9) a small shoulder can be observed on the low-field edge of the spectrum. This shoulder is largely obscured at higher microwave power (16 K, 0.013 mW), which indicates that this component of the spectrum saturates much more readily than the rest of the spectrum, that is, it has a slower electron spin relaxation rate. Even 0.8×10^{-3} mW is partially saturating the shoulder at 16 K but this is approximately the minimum power at which the spectrometer can maintain frequency lock. When the temperature is increased to 45 K the contribution of this low-field component to the spectrum is more clearly resolved and a g value of 2.000 can be estimated. With increasing temperature this peak evolves into the sharp signal with $g = 2.000$ that has been reported previously[8,9,13–18] in

(34) Penicaud, A.; Hsu, J.; Reed, C. A.; Koch, A.; Khemani, K. C.; Allemand, P.-M.; Wudl, F. *J. Am. Chem. Soc.* **1991**, *113*, 6698.
(35) Krusic, P. J.; Wasserman, E.; Parkinson, B. A.; Malone, B.; Holler, E. R., Jr. *J. Am. Chem. Soc.* **1991**, *113*, 6274.
(36) Rataiczak, R. D.; Koh, W.; Subramanian, R.; Jones, M. T.; Kadish, K. M. *Synth. Met.* **1993**, *55–57*, 3137.
(37) Rossing, R. G.; Danford, M. B. *Biometrics* **1968**, *24*, 117.
(38) Whittall, K. P.; Mackay, A. L. *J. Magn. Reson.* **1989**, *84*, 134.

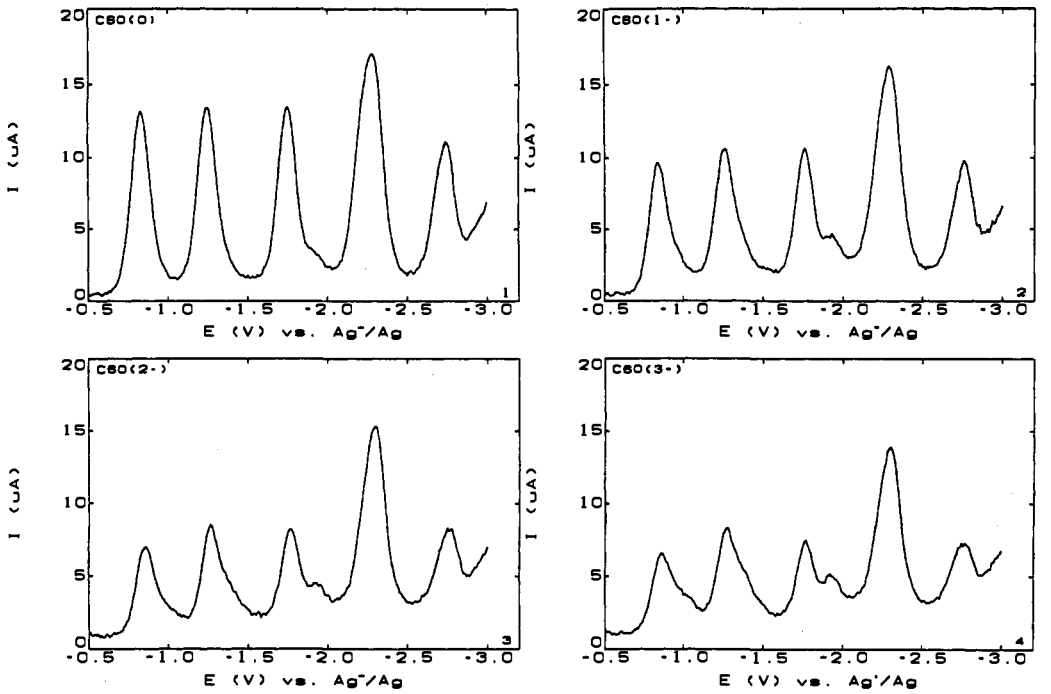

Figure 6. SWV at GC for (1) reduction of a solution of C_{60} and for C_{60} regeneration after bulk electrolysis at the Pt electrode to make (2) C_{60}^-, (3) C_{60}^{2-}, and (4) C_{60}^{3-}. The regeneration of C_{60} in the immediate vicinity of the electrode was performed by holding the electrode at –0.5 V for 20 s prior to initiating the voltage scans shown in parts 2–4.

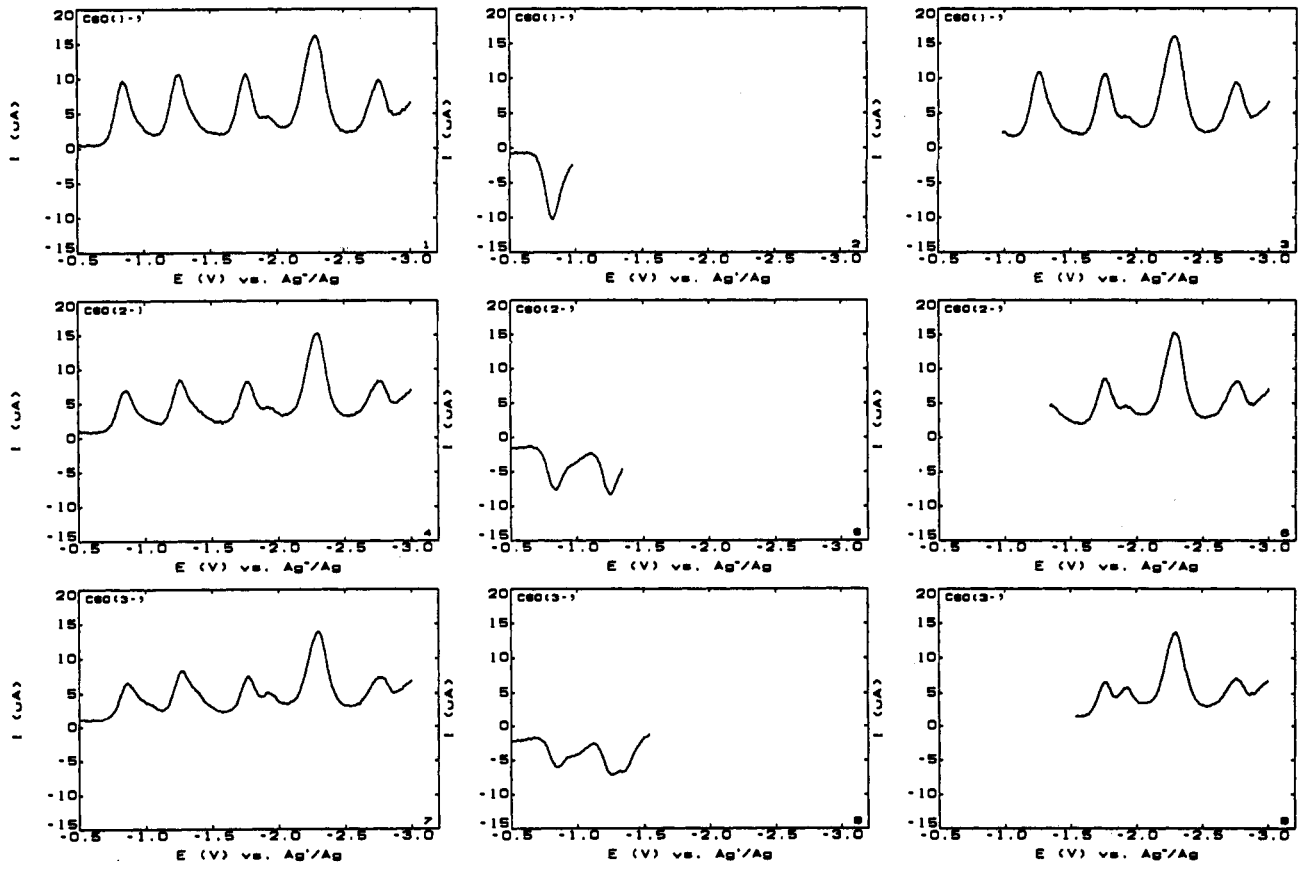

Figure 7. SWV at GC for C_{60} samples after bulk electrolysis at the Pt electrode to form C_{60}^- (blocks 1–3), C_{60}^{2-} (blocks 4–6), or C_{60}^{3-} (blocks 7–9). Sample in the immediate vicinity of the electrode was reduced to C_{60} by holding at –0.5 V for 20 s prior to initiating the reduction scans in blocks 1, 4, and 7. The oxidation scans shown in blocks 2, 5, and 8 or the reduction scans shown in blocks 3, 6, and 9 were recorded for the electrolyzed solutions, starting from the open cell potential.

C_{60}^- samples. In the 116 K spectra in Figure 9 the sharp signal at g = 2.000 is modulation broadened to facilitate observation of the underlying broad signal.

ESR Spectra of Samples Containing C_{60}^{2-}. The electrochemistry indicated that C_{60}^{2-} was generated and was relatively stable under the conditions of the electrochemistry experiment. The square wave data and NIR spectra indicated that 55–80% of the initial C_{60} was converted to C_{60}^{2-}. The characteristic red-orange color[13] of the sample was retained through all of the EPR spectroscopy, which also indicated the stability of the anion in the absence of oxygen. The EPR spectra of the samples of C_{60}^{2-} at 116 K (Figure 12B) showed a single sharp line. Similar sharp signals have been reported previously[13,15,16,18,19,36] for samples of C_{60}^{2-}.

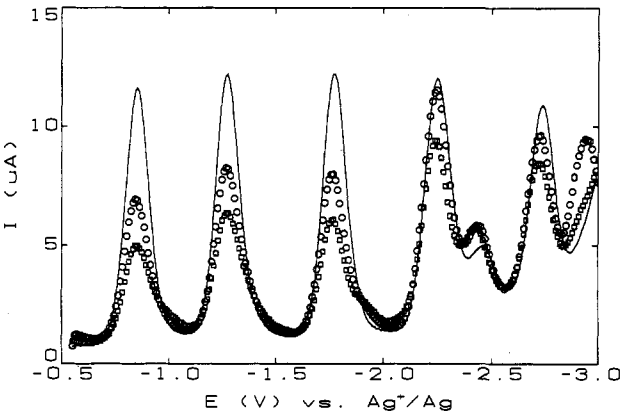

Figure 8. SWV at GC for a fresh solution of C_{60} (—), after bulk electrolysis to produce C_{60}^{3-} (□), and after bulk electrolysis to convert the C_{60}^{3-} back to C_{60}^{-} (○). For the C_{60}^{3-} and C_{60}^{-} solutions the C_{60} was regenerated at the surface of the electrode by holding the potential at –0.55 V for 20 s prior to initiating the reduction scan.

Double integration of the signals in several preparations gave radical concentrations that corresponded to 25–28% of the initial C_{60} concentration, assuming $S = {}^1/_2$. Since EPR signal intensity is proportional to $S(S+1)$, this same integral would correspond to only about 10% of the initial C_{60} concentration if the species had $S = 1$. When the spectrum of the same sample was recorded at a microwave power that partially saturated the sharp signal, additional peaks were observed with a splitting of about 12 G (Figure 12A). When the sample was cooled to about 7 K the sharp signal remained sharp (Figure 12C) and there was no evidence of splittings greater than about 12 G under a range of conditions of microwave power and magnetic field sweep width.

In an electron spin–echo experiment, the angle through which the net spin magnetization is turned by a microwave pulse is a function of the microwave magnetic field, B_1, and of the magnitude of the spin vector, S.[39] For example, for a sample with $S = 1$, the B_1 required for a 90° turning angle is smaller by a factor of $\sqrt{2}$ than that required for a sample with $S = {}^1/_2$. At 7 K, the B_1 required for a 90° pulse for the signal in the sample containing C_{60}^{2-} was the same as for the C_{60}^{-} sample, indicating that the sharp signal is due to species with $S = {}^1/_2$.

In studies of photoexcited $^3C_{60}$, zero-field splittings (ZFS) with $D = -0.0114$ cm^{-1} (122 G) have been observed at ca. 4 K.[40] Although the orbital occupancies of an $S = 1$ C_{60}^{2-} would be different than for the photoexcited triplet, one would expect the ZFS to be of the same order of magnitude, and we would have expected to be able to see the splitting in the spectra of C_{60}^{2-} at 7 K, if it had $S = 1$.

EPR Spectra of C_{60}^{3-}. The electrochemistry and NIR spectra indicated that under the conditions of these experiments C_{60}^{3-} was relatively unstable, which is consistent with the work of Dubois et al.[19] The EPR spectra of C_{60}^{3-} as a function of temperature as shown in Figure 13. At 7 K the EPR spectrum consists of a sharp signal at $g = 2.000$ superimposed on a broader anisotropic signal with $g_\perp = 1.997$ and $g_\parallel = 2.008$. The shape of the sharp signal at $g = 2.000$ changed little with increasing temperature. The apparent variations in the intensity of the $g = 2.000$ signal in Figure 13 are due to the selection of microwave power used to record the spectra. The $g = 2.000$ signal has much slower electron spin relaxation rates than the broader signals so it is partially saturated at the microwave powers that are appropriate to record the broader signals. As the temperature was increased from 7 to 55 K, the extrema of the broad signal moved closer together. However, above 77 K the signal broadened again. Although the samples for EPR spectroscopy were stored in liquid nitrogen, the highest integrated intensity observed at 116 K corresponded to only 21% of the initial C_{60} concentration, which is lower than the 40–50% observed by vis/NIR and electrochemistry during anion generation. There may have been significant decomposition during transfer to the EPR tube and prior to initial freezing of the sample. When a sample was held at room temperature for about 10 min and then refrozen, the spectrum shown in Figure 13A was observed, which showed only the sharp signal at $g = 2.000$, and there was no evidence of the broad signal. In view of the instability of the C_{60}^{3-}, it is proposed that the broad temperature-dependent signal is due to C_{60}^{3-} and the sharp signal is due to one or more other species. The increasing line width with increasing temperature for the C_{60}^{3-} signal has been observed previously[13,16,18] and the g value of 2.001 agrees with reports[13,16,36] for C_{60}^{3-}.

Saturation recovery experiments were performed on the broad C_{60}^{3-} signal between 8 and 25 K (Figure 14). The value of T_1 was about the same for the low-field and high-field portions of the signal. However, at each value of the magnetic field there was a wide distribution in relaxation rates. The relaxation rate was strongly temperature dependent, similar to what had been observed previously for C_{60}^{-}.[9] For both C_{60}^{-} and C_{60}^{3-}, the broad CW line widths above about 60 K are determined by rapid electron spin–lattice relaxation. The relaxation rates are dependent upon solvent and appear to be related to barriers to molecular motion.[9] These observations imply that the rapid motion of C_{60} species discussed below provides an efficient mechanism to couple electron spin energy to motional modes that provide a pathway to the lattice. C_{60} exhibits optical limiting properties that are due to rapid internal conversion of electronic energy to vibrational energy.[41,42]

Discussion

Dynamics of Photoexcited $^3C_{60}$ and C_{60} Anions. EPR studies of photoexcited $^3C_{60}$ by several groups have demonstrated that below about 20 K there is resolved ZFS with $D = -0.0114$ cm^{-1} (122 G) and $|E| = 0.00069$ cm^{-1}.[40] As the temperature is increased from 20 to 75 K, a dynamic process averages the ZFS. This process is assigned to interconversion between different Jahn–Teller distorted forms with nearly equal energy.[40] This is variously called dynamic Jahn–Teller distortion or pseudorotation. One would expect the dynamics of these processes to be similar for $^3C_{60}$ and for the anions studied here. It therefore seems reasonable to assign to the process between about 15 and 60 K, which averages the observed anisotropy of the EPR spectra for C_{60}^{-} and C_{60}^{3-}, to this same dynamic process (Figures 9 and 13).

Koga and Morokuma[20] performed *ab initio* calculations of the Jahn–Teller distortions for C_{60}^{-} and estimated that 6 equivalent D_{5d}, 10 equivalent D_{3d}, and 15 equivalent D_{2h} structures are nearly degenerate and are stabilized by about 2 kcal/mol relative to the symmetric I_h structure. They also made the important point that the addition of a single electron to such a large system will change the structure only slightly.[20] These calculations suggest that even at low temperature C_{60}^{-} probably exists in a distribution of geometries. This distribution in structures may be the source of the distribution in electron spin relaxation rates that was observed in the saturation recovery data. The near degeneracy of the distorted structures is consistent with the facile interconversion between them.

The line shape of the CW spectrum for C_{60}^{-} at 6 to 16 K has a sharp cutoff at low field and a broad wing to high field. There are three significant features of the high-field wing of the spectrum. (1) In this portion of the signal the spin–lattice relaxation rate, $1/T_1$, is fastest. (2) The electron spin phase memory relaxation rate, $1/T_m$, is fastest in this region of the spectrum. (3) The intensity in the wing is greater than would be expected for a Gaussian broadening around the high-field extrema. Even in this portion of the spectrum the line width is not relaxation rate determined ($T_m = 0.3$ μs corresponds to a spin-packet line width, ΔB_{pp}, of 0.2 G), so other effects determine the line width. One source of line broadening would be variation in g values due to Jahn–Teller distortion. The structures with the least distortion from I_h symmetry are expected to have g values furthest from 2.002 and to have the fastest electron spin relaxation rates. Thus the low-temperature line shape may reflect the distribution in Jahn–Teller distortions. Since a relatively small number of structures may be populated, the distribution may not be Gaussian. One would also expect that as distortions became more extensive the g value would approach a limiting value, characteristic of a C_{60} radical with a more localized unpaired electron spin. Such

(39) Sloop, D. J.; Yu, H.-L.; Lin, T.-S.; Weissman, S. I. *J. Chem. Phys.* **1981**, *75*, 3746.

(40) Regev, A.; Gamliel, D.; Meiklyar, V.; Michaeli, S.; Levanon, H. *J. Phys. Chem.* **1993**, *97*, 3671. References to the earlier work on $^3C_{60}$ are given in this paper.

(41) Tutt, L. W.; Kost, A. *Nature* **1992**, *356*, 225.

(42) Wurz, P.; Lykke, K. R. *J. Phys. Chem.* **1992**, *96*, 10129.

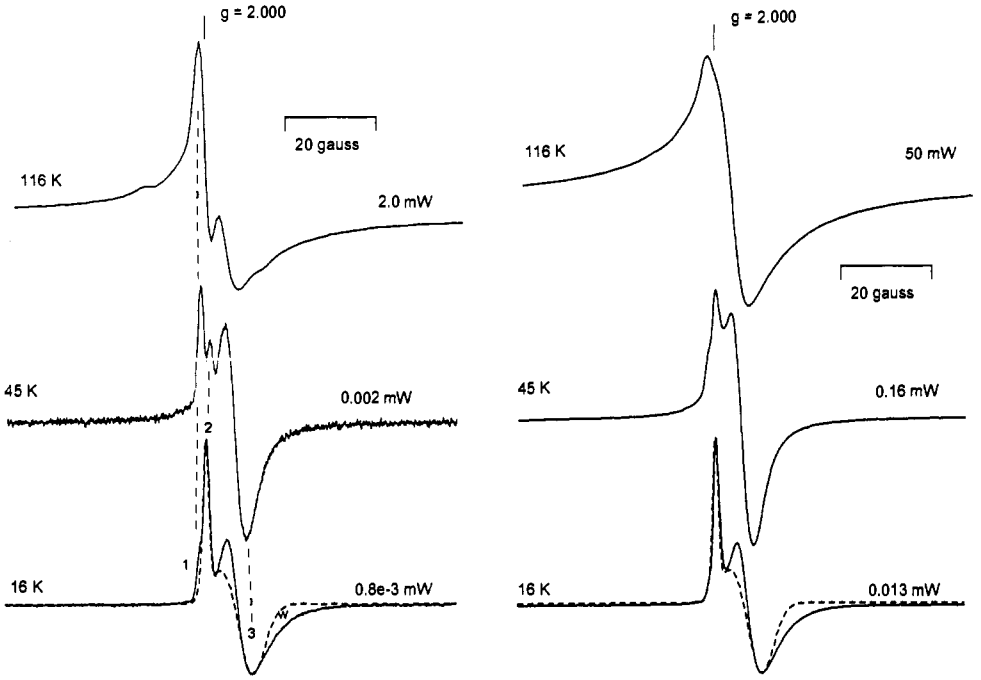

Figure 9. CW EPR spectra (100 G scans) of C_{60}^- in frozen toluene–acetonitrile solution as a function of temperature and microwave power at 9.3898 GHz (116 K) or 9.2339 GHz (16 and 45 K). Spectra taken at different frequencies were shifted horizontally to align corresponding g values. At each temperature a lower power spectrum is shown on the left and a higher power spectrum is shown on the right. The microwave power is shown to the right of each spectrum. The modulation amplitude was 4.0 G at 116 K and 0.16 G at 45 and 16 K. The simulated spectra (– –) were calculated for $g_\perp = 1.9937$ and $g_\parallel = 1.9987$ and anisotropic line widths: $\sigma_\perp = 6.2$ G, $\sigma_\parallel = 1.0$ G.

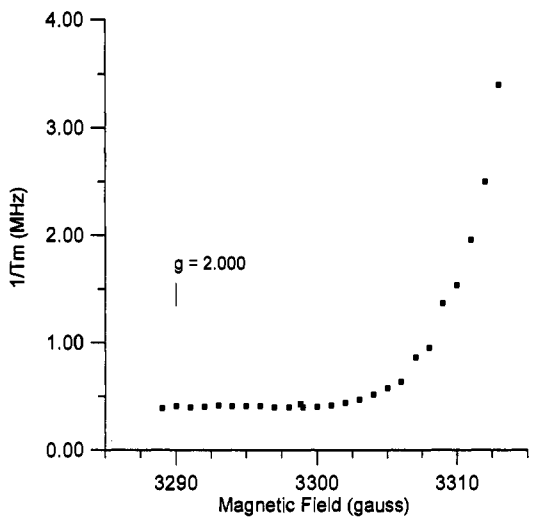

Figure 10. Magnetic field dependence of $1/T_m$ for C_{60}^- in frozen toluene–acetonitrile solution at 15 K and 9.2089 GHz. Spin–echo data were fit to a single exponential with an exponent of 1.0.

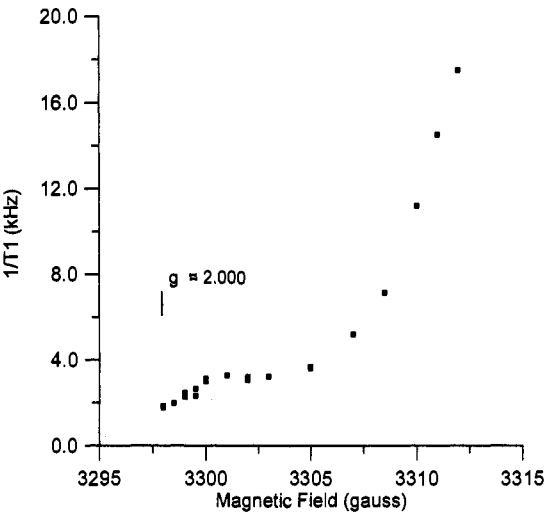

Figure 11. Magnetic field dependence of $1/T_1$ for C_{60}^- in frozen toluene–acetonitrile solution at 8 K and 9.2321 GHz. Saturation recovery data were fit to a single exponential.

a distribution could have a relatively sharp cutoff at the limiting value, which appears to be about 2.000. The distribution in g values and relaxation rates also may be impacted by differences in ion pairing and/or solvation.[8,9]

Jahn–Teller Splitting for C_{60}^{2-}. There is on-going disagreement in the literature concerning the spin state of C_{60}^{2-}. Molecular orbital calculations predict that addition of an electron to the triply degenerate LUMO of C_{60} will result in Jahn–Teller distortion that splits the set of three orbitals into one at lower energy and a pair at higher energy.[20,21] Addition of a second electron would produce a diamagnetic dianion. However, there have been reports[13,15,16,18,19,36] of EPR signals for C_{60}^{2-}, which led to the assignment of an $S = 1$ state for C_{60}^{2-} [8,13,16,19] and the proposal that the Jahn–Teller splitting was the inverse of that suggested by calculations.[8]

Since dynamic averaging of the anisotropy of the $S = 1$ signal for photoexcited $^3C_{60}$ has been observed to give a sharp signal above about 100 K and in fluid solution,[40,43] it might be argued that the sharp signal shown in Figure 12 and reported by other authors[13,15,16,18,19] could be due to dynamic averaging of the ZFS for $S = 1$ C_{60}^{2-}. However, if that were the case, one would expect the signal attributed to C_{60}^{2-} to broaden at low temperature, analogous to what is observed for photoexcited $^3C_{60}$. As shown in Figure 12C, such broadening was not observed for the samples examined in this study.

It has also been proposed that weaker lines in the spectra of C_{60}^{2-} with splittings of 13 and 28 G at 120–226 K[13,16,19] and of 54 G at 130 K[16] are due to the ZFS for $S = 1$ dianion. In our samples we have observed that the ca. 13 G splittings collapse only when the solvent melts.[9] If dynamic averaging processes are occurring for C_{60}^{2-} at rates comparable to what was observed

(43) Steren, C. A.; Levstein, P. R.; van Willigen, H.; Linschitz, H.; Biczok, L. *Chem. Phys. Lett.* **1993**, *204*, 23.

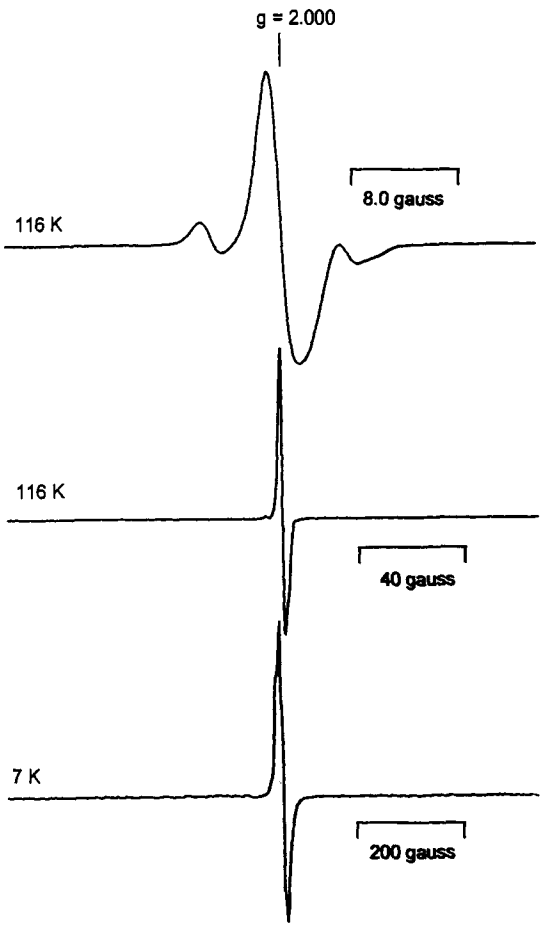

Figure 12. Temperature dependence of the CW EPR spectra of a sample containing C_{60}^{2-} in frozen toluene–acetonitrile solution at 9.3893 (116 K) and 9.2377 GHz (7 K): (A) 116 K, 40 G scan, 1.0 G modulation amplitude, and 50 mW microwave power; (B) 116 K, 200 G scan, 1.0 G modulation amplitude, and 0.04 mW microwave power; (C) 7 K, 1000 G scan, 4.0 G modulation amplitude, and 1.0 mW microwave power. Spectra taken at different frequencies and sweep widths were shifted horizontally to align at $g = 2.000$. Labeling top to bottom is A to C.

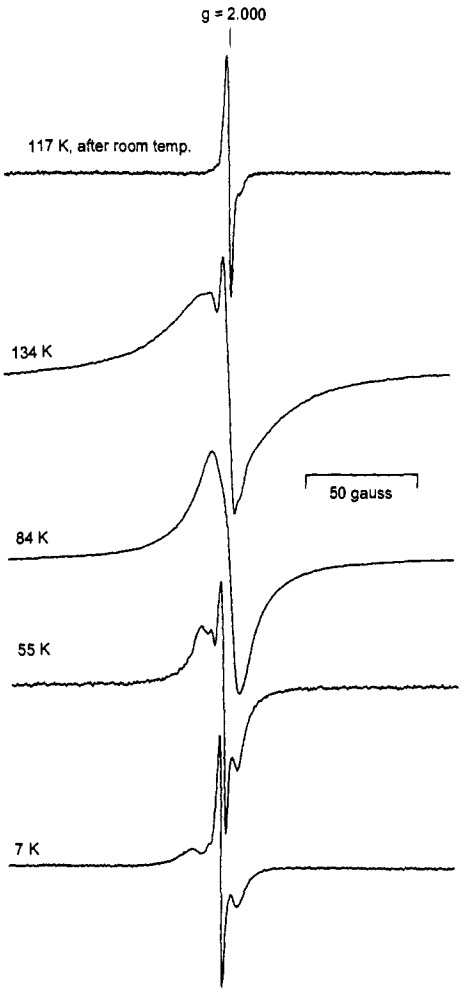

Figure 13. Temperature dependence of the CW EPR spectra (200 G scans) of C_{60}^{3-} in frozen toluene–acetonitrile solution. (A) Spectrum of a sample left to stand at room temperature for about 15 min then re-frozen: obtained at 9.3895 GHz with 0.04 mW microwave power and 1.0 G modulation amplitude. Spectrum of fresh sample: (B) obtained at 9.3878 GHz with 20 mW microwave power and 4.0 G modulation amplitude; (C) obtained at 9.1046 GHz with 20 mW microwave power and 4.0 G modulation amplitude; (D) obtained at 9.2331 GHz with 0.015 mW microwave power and 1.0 G modulation amplitude; (E) obtained with 9.2331 GHz with 0.15×10^{-3} mW microwave power and 1.0 G modulation amplitude. Spectra taken at different frequencies were shifted horizontally to align corresponding g values. Labeling top to bottom is A to E.

for $^3C_{60}$, C_{60}^-, and C_{60}^{3-}, splittings of 12–50 G would be largely averaged at the temperatures where these splittings are attributed to C_{60}^{2-}. Since it seems unlikely that the dynamics of Jahn–Teller distortions would be dramatically different for the dianion than for the monoanion and the trianion, the assignment of these splittings to C_{60}^{2-} is suspect. A tumbling correlation time for C_{60} of 9.1 ps at 283 K was obtained by solid-state NMR.[44] Other techniques have also shown low barriers to rotation for C_{60}.[45,46] Molecular rotation of C_{60}^{2-} is also likely to be fast enough to average splittings of the order of 20–50 G well before the melting point of the solvent. These arguments lead to the conclusion that the species which gives rise to the splittings of 13–50 G that are not collapsed by dynamic processes at 100–200 K must have lower symmetry and/or higher barriers to rotation than C_{60} and these signals are probably not due to C_{60}^{2-}. Suspicions that these signals are not due to C_{60}^{2-} are increased by (a) the observation that the radical at 7 K requires microwave power for a 90° pulse characteristic of an $S = {}^1/_2$ system and by (b) the low integrals of the EPR spectra. We propose that C_{60}^{2-} is diamagnetic, and the EPR signals that are observed in samples that are prepared to contain C_{60}^{2-} are due to one or more other species.

Mehran et al.[10] prepared C_{60}^{n-} by reaction of C_{60} with elemental K in THF with subsequent evaporation of the solvent and observed that the intensity of the EPR signal in the solid was maximum for $n \sim 1$ and decreased with further reduction. They proposed that the −2 anion is diamagnetic.[10]

Proposed Assignment of Sharp Signals in EPR Spectra of C_{60} Anions. A persisting puzzle is the nature of the species that give rise to the EPR signals observed in the spectra of the C_{60} anions. Since sharp EPR signals are observed in samples prepared to contain the C_{60}^-, C_{60}^{2-}, and C_{60}^{3-} anions, and some of the sharp signals appear to have multiple components, there may be more than one source of these signals.

In an early report Greaney and Gorun[17] proposed that there was rapid electron transfer between neutral C_{60} and C_{60}^- and assigned the sharp EPR signal to "free" C_{60}^- and the broad signal to ion-paired C_{60}^-. Reed and co-workers[8] pointed out that both signals were observed in frozen solution where electron transfer would be slow and that the EPR spectrum was not impacted by deliberate addition of neutral C_{60}, which argues against the earlier assignment. Dubois et al. proposed that the sharp signal was due to C_{60}^{2-} produced by disproportionation.[13] Reed and co-workers[8]

(44) Johnson, R. D.; Yannoni, C. S.; Dorn, H. C.; Salem, J. R.; Bethune, D. S. *Science* **1992**, *255*, 1235.
(45) Neumann, D. A.; Copley, J. R. D.; Cappellitti, R. L.; Kamitakahara, W. A.; Lindstrom, R. M.; Creegan, K. M.; Cox, D. M.; Romanow, W. J.; Coustel, N.; McCauley, J. P., Jr.; Maliszewskyj, N. C.; Fischer, J. E.; Smith, A. B., III *Phys. Rev. Lett.* **1991**, *67*, 3808.
(46) Shi, X. D.; Kortan, A. R.; Williams, J. M.; Kini, A. M.; Savall, B. M.; Chaikin, P. M. *Phys. Rev. Lett.* **1992**, *68*, 827.

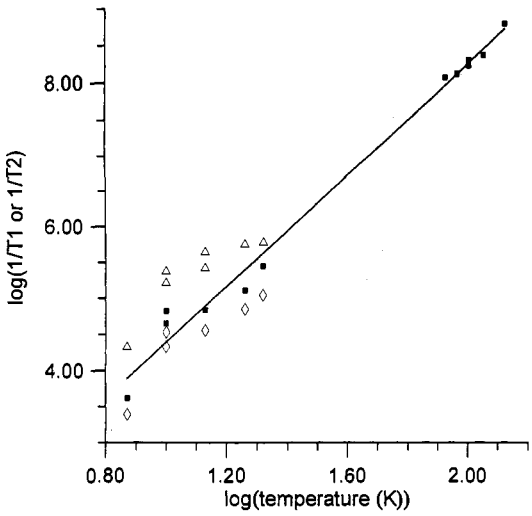

Figure 14. Temperature dependence of electron spin relaxation rates for C_{60}^{3-} in frozen toluene–acetonitrile solution at 9.2328 GHz and 3290 G. Saturation recovery data between 5 and 25 K were fit to a single exponential (■) or to a sum of two exponentials with a slow (◇) and a fast (△) component. Between 84 and 134 K, $1/T_2$ (■) was determined from the temperature-dependent contribution to the CW line width. The solid line is a least-squares fit to the average $1/T_1$ data at low temperature and the $1/T_2$ data at high temperature. The slope (3.86) is a measure of the temperature dependence of the relaxation rates.

argued that disproportionation was unlikely to account for the intensity of the sharp signal. Boulas et al. subsequently showed that the intensity of the sharp signal increased when the solution was made more reducing, consistent with the assignment to C_{60}^{2-}.[15] However, their observation does not rule out the possibility that the sharp signal is due to another species with a reduction potential similar to that for C_{60}^{2-} or produced from C_{60}^{2-}. As discussed above, the sharp signals observed in our samples do not exhibit the characteristics expected for C_{60}^{2-} at low temperature.

Reed and co-workers[8] observed that the intensity of the sharp signal in the spectra of C_{60}^- appeared to increase with increasing temperature and proposed that it was due to a thermally accessible excited state. However, the caption to the figure that displays their spectra states that the microwave power was 126 mW. As shown in Figure 9, the apparent intensity of the sharp signal in the C_{60}^- spectra is strongly dependent on microwave power. The high power used in ref 8 would have drastically saturated the sharp signal at lower temperatures. The reported change in signal intensity with temperature is probably due to partial relief of microwave power saturation with increasing temperature. Even the spectrum of C_{60}^- is likely to have been significantly distorted by the use of such high microwave power at the lower temperatures shown in Figure 2 of ref 8.

Samples prepared in various labs may have different sources of the sharp signals; however, none of the proposals made to date appear convincing. We suggest that alternate assignments need to be considered.

Explanations of the sharp signals in the EPR spectra need to account for the fact that the lines remain relatively sharp over wide temperature ranges (ca. 5–300 K) and have much slower electron spin relaxation rates than the signals for C_{60}^- and C_{60}^{3-}. These observations suggest that the species which give rise to these signals have lower symmetry and higher barriers to molecular rotation than C_{60}. These changes could arise from substitution of the C_{60}. The substituent would make the barrier to molecular motion much higher than in the nearly-spherical C_{60}. The lower symmetry would result in splitting of the degeneracy of the C_{60} LUMO. The loss of orbital degeneracy and slower molecular motion would account for the sharper lines and slower electron spin relaxation. It seems reasonable to examine what substitution processes might be occurring.

Morton and co-workers have examined reactions in which an organic radical (R) adds to C_{60} forming a $C_{60}R$ radical in which the unpaired electron is largely localized on the carbons adjacent to the point of substitution.[47,48] The EPR spectra of these radicals exhibit narrow lines with g values between 2.0022 and 2.0025. These systems demonstrate that in the limit where an unpaired electron on a C_{60} derivative is localized, the g values are close to that of the free electron (2.0023), as is typical of many organic radicals. The sharper lines for these radicals than for C_{60}^- are consistent with the expectation that lowering the symmetry results in slower electron spin relaxation rates. However, the g values for alkyl-substituted C_{60} radicals are higher than for the sharp (g = 2.000) signal observed in the C_{60} anion spectra so they do not appear to be plausible assignments.

One impurity that is likely to be present in most preparations of C_{60} anions is traces of water. The preparations of a fulleride oxide[49] and that of hydroxy fullerides[50] have been reported. Since reduction potentials for these derivatives and g values for the resulting radicals have not been reported, it is difficult to assess whether these are plausible sources of the observed EPR signals. $C_{60}H_n$[51] and $C_{60}H_2$[52] have also been reported. If radicals derived from these species were responsible for the sharp EPR signals, one would expect to see increased proton modulation in the electron spin–echo data for the sharp signal. However, the proton modulation of the electron spin echoes for the sharp signal at 10 K was similar to that observed for C_{60}^- and C_{60}^{3-}, and is probably due to solvent protons. Thus, hydrogenation does not appear to be a plausible explanation.

The organic radical derivatives of C_{60} have a strong tendency to dimerize.[47,48] The enthalpy of dimerization increases as the steric requirements of the R group decrease. The largest enthalpy of dimerization reported is 35.5 kcal/mol for R = isopropyl. Photopolymerization has also been observed for solid C_{60} films.[53] These observations suggest the possibility of dimerization of C_{60}^- to form $(C_{60})_2^{2-}$, which would be diamagnetic. One-electron reduction of this dimer would have a single unpaired electron, a reduced symmetry, and a greatly increased barrier to interconversion of Jahn–Teller distortions and to rotation of the molecule as a whole. The g value of such a species might be close to that observed (2.000) for the low-field extrema of the C_{60}^- spectrum, which was proposed above to be due to the structure with the largest Jahn–Teller distortion. It would be expected to have a relatively sharp signal and could be one source of the sharp signal that is observed in the spectra of the C_{60} anions. Such species or higher polymers might account for the report that the sharp signal in spectra of C_{60}^- was larger at more reducing potentials.[15] Since there would probably be relatively weak electronic interaction between the two halves of the dimer, it would also seem plausible that a further reduction could occur to produce a biradical with one unpaired electron on each half of the dimer. This species could account for the reported splittings of 12–50 G that are not averaged by dynamic processes above 100 K. The assignment of a weak signal to an impurity or byproduct is difficult. The actual assignment or assignments may be different from any

(47) Morton, J. R.; Preston, K. F.; Krusic, P. J.; Wasserman, E. *J. Chem. Soc. Perkin Trans 2* **1992**, 1425.
(48) Morton, J. R.; Preston, K. F.; Krusic, P. J.; Hill, S. A.; Wasserman, E. *J. Am. Chem. Soc.* **1992**, *114*, 5454.
(49) Creegan, K. M.; Robbins, J. L.; Robbins, W. K.; Millar, J. M.; Sherwood, R. D.; Tindall, P. J.; Cox, D. J. *J. Am. Chem. Soc.* **1992**, *114*, 1103.
(50) Chiang, L. Y.; Swirczewski, J. W.; Hsu, C. S.; Chowdhury, S. K.; Cameron, S.; Creegan, K. *J. Chem. Soc. Chem. Commun.* **1992**, 1791.
(51) Haufler, R. E.; Conceicao, J.; Chibante, L. P. F.; Chai, Y.; Byrne, N. E.; Flanagan, S.; Haley, M. M.; O'Brien, S. C.; Pan, C.; Xiao, Z.; Billups, W. E.; Ciufolini, M. A.; Hauge, R. H.; Margrave, J. L.; Wilson, L. J.; Curl, R. F.; Smalley, R. E. *J. Phys. Chem.* **1990**, *94*, 8634.
(52) Henderson, C. C.; Cahill, P. A. *Science* **1993**, *259*, 1885.
(53) Rao, A. M.; Zhou, P.; Wang, K.-A.; Hager, G. T.; Holden, J. M.; Wang, Y.; Lee, W.-T.; Bi, X.-X.; Eklund, P. C.; Cornett, D. S.; Duncan, M. A.; Amster, I. J. *Science* **1993**, *259*, 955.

that have been proposed. However, it seems unlikely that any of the previously published assignments for the sharp signal(s) are correct.

Conclusions

SWV is a convenient method to monitor the efficiency of C_{60} anion production. Dynamic averaging of anisotropy in EPR spectra occurs in a similar temperature range (15–60 K) for $^3C_{60}$, C_{60}^{-1}, and C_{60}^{3-}, which suggests that dynamic Jahn–Teller distortions are operative in all three cases. Electron spin–lattice relaxation is temperature dependent and determines the EPR line widths for C_{60}^{-} and C_{60}^{3-} above about 70 K. The dianion of C_{60} is diamagnetic. Substituted derivatives of C_{60} may be the source of the sharp EPR signals observed in samples prepared to contain C_{60}^{-}, C_{60}^{2-}, and C_{60}^{3-}.

Acknowledgment is made to the donors of the Petroleum Research Fund, administered by the American Chemical Society, for partial support of this research.